

Polymer Chemistry

Accepted Manuscript

This article can be cited before page numbers have been issued, to do this please use: P. Manini, V. Lino, G. D'Errico, S. Reale, A. Napolitano, F. De Angelis and M. d'Ischia, *Polym. Chem.*, 2020, DOI: 10.1039/D0PY00700E.



This is an Accepted Manuscript, which has been through the Royal Society of Chemistry peer review process and has been accepted for publication.

Accepted Manuscripts are published online shortly after acceptance, before technical editing, formatting and proof reading. Using this free service, authors can make their results available to the community, in citable form, before we publish the edited article. We will replace this Accepted Manuscript with the edited and formatted Advance Article as soon as it is available.

You can find more information about Accepted Manuscripts in the [Information for Authors](#).

Please note that technical editing may introduce minor changes to the text and/or graphics, which may alter content. The journal's standard [Terms & Conditions](#) and the [Ethical guidelines](#) still apply. In no event shall the Royal Society of Chemistry be held responsible for any errors or omissions in this Accepted Manuscript or any consequences arising from the use of any information it contains.

ARTICLE

“Blackness” is an index of redox complexity in melanin polymers

Paola Manini,^{*a} Valeria Lino,^{a,b} Gerardino D’Errico,^a Samantha Reale,^c Alessandra Napolitano,^a Francesco De Angelis,^c Marco d’Ischia^aReceived 00th January 20xx,
Accepted 00th January 20xx

DOI: 10.1039/x0xx00000x

Disclosed herein is the first experimental evidence for a direct correlation between the broadband visible light absorption (“blackness”) and the coexistence of reduced and oxidized substructures in a set of model polymers from isomeric dihydroxynaphthalenes structurally related to fungal melanin (mycomelanin) from 1,8-dihydroxynaphthalene. Excellent linear plots ($r^2 = 0.97$ and 0.94) were determined between the integrals of featureless absorbance curves over the 400–800 nm range, the electron spin density values in the EPR spectra and the width of selected oligomer peak clusters in the MALDI-MS spectra. Blackness, which is shown to be strongly interrelated with electron spin density, is thus proposed herein as a robust index of redox inhomogeneity and electron complexity reflecting the shift of oligomer populations toward highest oxidation states.

Introduction

Melanins, a characteristic group of insoluble phenolic polymers found widespread in Nature from humans to mammals, plants and fungi, display typical dark colorations and an outstanding combination of optoelectronic,¹ free radical,² antioxidant,³ metal chelating⁴ and semiconductor-like properties⁵ that raise considerable interest for manifold applications in materials science and biomedicine.^{6–9} Although commonly implicated in the photoprotective role of the nitrogenous eumelanins¹⁰ and in the radioprotective capacity of the nitrogen free allomelanins in certain fungi, i.e. *Aspergillus fumigatus* or *Cladosporium sphaerospermum*,¹¹ the origin of the black chromophore, that is the “blackness”, is still unclear. The variable degree of blackness that characterizes both natural and synthetic melanins has traditionally been suggested to reflect a complex interplay of interrelated structural factors rooted in different levels of chemical disorder.^{12,13} In particular, the darker colors have been ascribed to excitonic effects reflecting strong intermolecular perturbations between the various chromophoric components sustained by efficient aggregation.^{14–17} In support of this view, model studies on a soluble eumelanin-like polymer produced by oxidation of glycated 5,6-dihydroxyindole (DHI) units have shown that the intensity of the visible chromophore depends on the coexistence of reduced and oxidized units and is a function of concentration/aggregation.¹⁴

Transient spectral hole burning, a manifestation of high chemical heterogeneity, has recently been detected by means of femtosecond broadband transient absorption spectroscopy on DOPA melanin.¹⁷

Besides traditional model polymers from DOPA or DHI, a valuable yet little investigated platform for inquiring into the origin of melanin chromophore is provided by synthetic fungal allomelanin (mycomelanin) mimics produced by oxidative polymerization of 1,8-dihydroxynaphthalene (1,8-DHN) and related precursors. Studies of 1,8-DHN polymers have shown a deep black color associated with an unusually intense EPR signal and potent antioxidant effects, far exceeding those of the nitrogenous eumelanin from DHI.¹⁸ Studies of the structure, properties and mechanism of formation of 1,8-DHN mycomelanin led to the identification of the main oligomer intermediates, displaying the 2,2’-, 2,4’, and 4,4’-coupling patterns (Figure 1), a chemistry reflecting the reactivity of transient phenoxyl radical intermediates.^{19,20}

Recently, a re-examination of melanin properties has led to a revisitation of the traditional chemical disorder paradigm in terms of a more sophisticated model based on interrelated levels of chemical complexity, which however has not yet been assessed within a solid framework of quantitative structure-property relationship.²¹

As an attempt to fill this gap, we investigated herein a set of synthetic melanin polymers produced from isomeric dihydroxynaphthalenes (DHNs) with a view of highlighting possible correlations between visible absorption properties, electron spin density and oligomer redox states. Aim of the study was to probe whether “blackness”, a typical feature of melanins, can be qualified as an emergent property associated with redox disorder and can thus be regarded as an index of π -electron complexity underlying most physicochemical properties and biological roles.

^a Department of Chemical Sciences, University of Napoli Federico II, Complesso Universitario Monte S. Angelo, via Cintia 4, I-80126, Napoli, Italy.
pmanini@unina.it

^b Scuola Normale Superiore, Piazza dei Cavalieri 7, I-56126 Pisa, Italy.

^c Department of Physical and Chemical Sciences, University of L’Aquila, Via Vetoio Coppito, I-67100, L’Aquila, Italy.

Electronic Supplementary Information (ESI) available: UV-vis, ATR, MALDI and EPR spectra of the synthetic mycomelanins (powder and thin films). See DOI: 10.1039/x0xx00000x

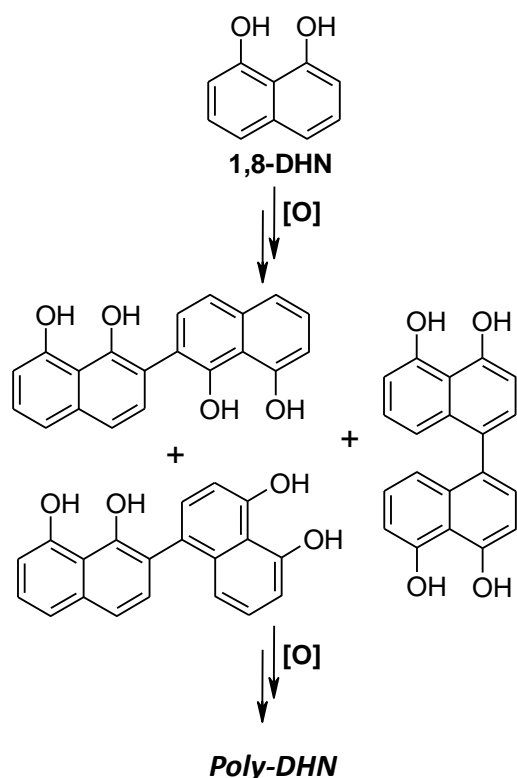


Figure 1. First stages of the oxidative polymerization of 1,8-DHN.

Results and discussion

DHN substrates for melanin synthesis included, besides naturally occurring 1,8-DHN, 1,6-dihydroxynaphthalene (1,6-DHN), 2,7-dihydroxynaphthalene (2,7-DHN) and 2,6-dihydroxynaphthalene (2,6-DHN), the only one generating an inter-ring quinone, whereas those producing intra-ring quinones (i.e. 1,2-DHN and 1,4-DHN) were not considered because of the expectedly different chemistry. Polymers from 1-naphthol (1-HN) and 2-naphthol (2-HN) were also included as reference materials for structure-property relationship (Figure 2).

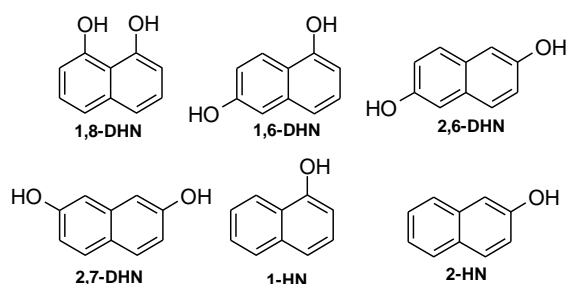


Figure 2. Selected (di)hydroxynaphthalenes.

The mode of polymerization of the isomeric DHNs was initially investigated via spectrophotometric analysis of the oxidation reactions. The latter were conducted by a standard biomimetic protocol involving the oxidation of the substrate with the

horseradish peroxidase (HRP)/H₂O₂ system in 0.1 M phosphate buffer at pH 7.0.¹⁹

DOI: 10.1039/D0PY00700E

The spectrophotometric analysis revealed marked differences both in the rate of development and nature of the resulting chromophores, in line with broadly different chemistries. In particular, while 1,6-DHN exhibited an oxidative behaviour quite similar to that of 1,8-DHN,²⁰ leading to the rapid development of a dark coloration associated with the formation of absorption maxima set in the 400–700 nm region, 2,7- and 2,6-DHN underwent a slower oxidation process with the development of an absorption maximum centered around 400 nm and long tails in the visible spectrum (see ESI Section). After 24 h reaction time, synthetic melanins were collected and a similar procedure was adopted also for the reference compounds 1-HN and 2-HN.

Visual inspection of the polymers indicated three different types of colorations, namely: a) dark-brown (poly-1,6-DHN and poly-1,8-DHN); b) deep coloration, e.g. bluish-green (poly-2,7-DHN) or violet (poly-1-HN); and c) light-colorations (poly-2,6-DHN and poly-2-HN) (Figure 3: insets). In agreement with the visual characteristics, poly-1,8-DHN and poly-1,6-DHN exhibited the typical melanin-like broadband absorption profiles, poly-2,7-DHN and poly-1-HN showed intense maxima in the UV and a low absorption in the visible region of the spectrum whereas poly-2,6-DHN and poly-2-HN showed intense maxima only in the UV region of the spectrum (see ESI section).

To investigate the absorption properties of the synthetic melanins under conditions devoid of significant scattering effects, the chromophore development was monitored during the formation of melanin thin films by ammonia induced solid state polymerization (AISSP).^{22,23} This procedure involves the exposure of DHN thin films, produced by spin coating from methanol solutions, to an ammonia atmosphere equilibrated with air to induce autoxidative polymerization in the solid state. After 24 h the polymerization was complete and each of the thin film, exhibiting quite similar thickness (see ESI Section), was subjected to spectrophotometric analysis.

As shown in Figure 3, after exposure to ammonia vapors only the thin films from 1,6-DHN developed the typical dark brown coloration of melanin polymers, as previously reported in the case of 1,8-DHN.²² On the other hand, the spectra from 2,7- and 2,6-DHN melanin thin films revealed the presence of the same absorption maxima of the starting DHNs derivatives with an appreciable growth in the absorbance around 400 nm along with long tails in the visible region of the spectrum. These results confirmed different reaction pathways for the oxidative polymerization process of the various DHNs tested both in solution and in the solid state.

To integrate the spectroscopic characterization of the synthetic melanin polymers, EPR spectra were recorded on the solid polymer sample. Data reported in Table 1 showed that the g-factor values for all the polymers were slightly lower than those measured for nitrogenous eumelanins from DHI and DHICA, suggesting a more pronounced C-centered radical character in the fungal melanin mimics. This difference is likely due to the lack of *o*-semiquinone moieties in the former polymers. Moreover, significant differences were evident for the spin

density values of the DHN melanins examined despite no appreciable variation in the ΔB values.

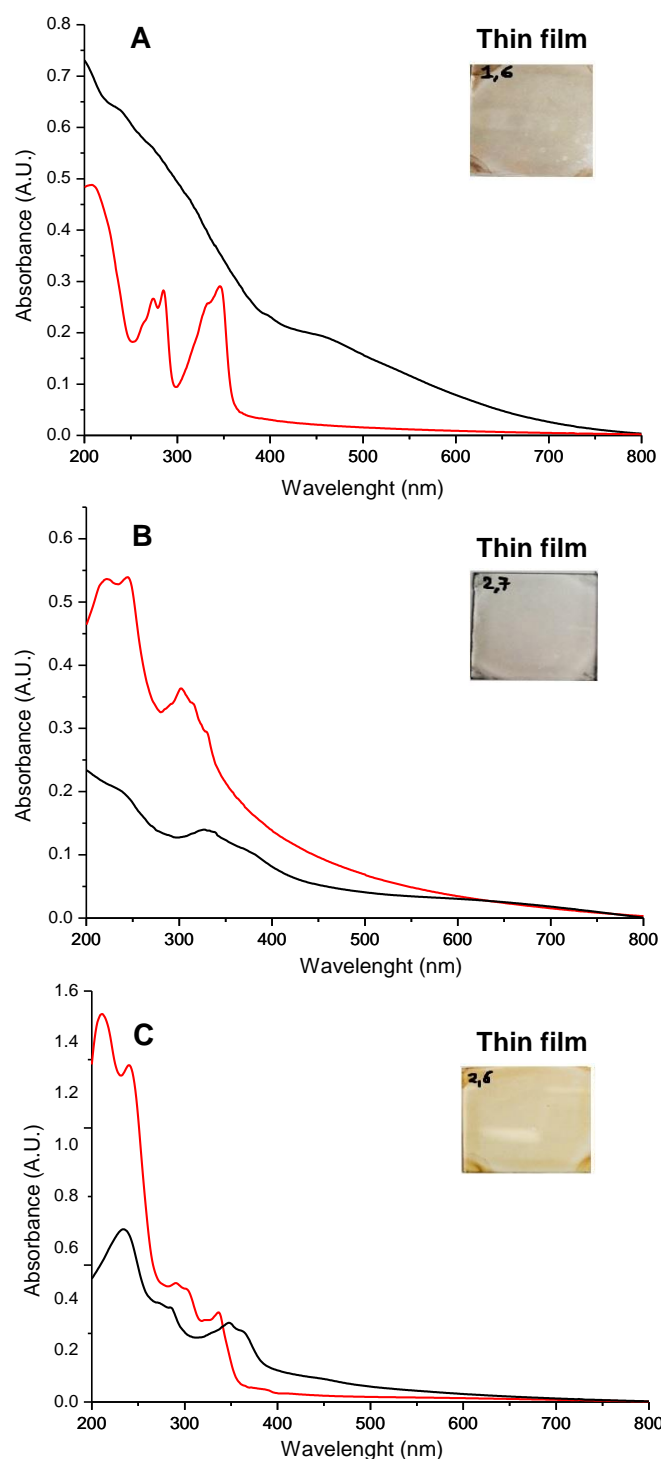


Figure 3. UV-visible spectra of 1,6-DHN (A), 2,7-DHN (B) and 2,6-DHN (C) thin films on quartz before (red trace) and after (black trace) AISSP. The insets show pictures of the thin films.

Notably, very intense signals, exceeding that of DHI melanin, were recorded for poly-1,6-DHN and poly-1,8-DHN, with spin density values close to 10^{19} spin/g whereas a relatively weak signal with a spin density of 7.5×10^{15} spin/g was registered in the case of poly-2,6-DHN.

Table 1. EPR parameters of synthetic melanins. Experimental uncertainties are ± 0.0003 on g-factor, $\pm 10\%$ on spin density and ± 0.2 G on ΔB . DOI: 10.1039/D0PY00700E

Synthetic mycomelanins	g-factor	ΔB (G)	Spin density (spin / g)
Poly-1,8-DHN ¹⁸	2.0030	4.8	8.1×10^{18}
Poly-1,6-DHN	2.0030	4.8	9.1×10^{18}
Poly-2,7-DHN	2.0030	4.6	5.6×10^{17}
Poly-2,6-DHN	2.0027	4.8	7.5×10^{15}
Poly-1-HN	2.0030	4.0	2.1×10^{17}
Poly-2-HN	2.0032	5.2	2.8×10^{18}

A first inspection of the data collected from these sets of analyses pointed to similar trends with regards to blackness and electron spin density, suggesting a common background of redox and electronic properties in the oligomer π -systems. On this basis, the existence of possible correlations between the optical and paramagnetic properties of DHN melanins and the redox state of the oligomer components was investigated.

To this aim, MALDI-MS spectra were then recorded for all melanins examined, both on bulk polymers and in films produced by AISSP (see ESI section). The results were in line with those reported in previous studies on the synthetic 1,8-DHN polymer^{18,19} and on the 1,8-DHN-based allomelanin extracted from *M. fijiensis*.²⁴ Largely regular patterns of oligomers with a repeating unit of 158 Da and matching series of $[M+Na]^+$ and $[M+K]^+$ species were detected for all polymers, up to the 13-mer in the case of poly-1,6-DHN and poly-1,8-DHN. A lower degree of polymerization was apparent in the case of poly-2,6-DHN and poly-2,7-DHN, not exceeding the 10-mer as the last detectable level. These latter were the melanins with the lighter coloration and lower spin density levels.

All spectra denoted a relative structural integrity of the polymers, a feature which is usually not observed in the case of synthetic indole-based eumelanins from DHI and DHICA.²⁵⁻²⁷ Likewise, poly-1-HN and poly-2-HN showed sequential patterns of peaks (up to the 15-mer) separated by 142 Da, relative to $[M+H]^+$ species.

Closer inspection of the clusters in the MALDI mass spectra revealed however subtle but significant differences among the polymers and provided important information on their redox state and behavior. In particular, in the case of poly-1,6-DHN and poly-1,8-DHN each cluster was made of pseudomolecular ion peaks ($[M+Na]^+$), for the fully reduced oligomeric structures, accompanied by peaks at lower m/z values, compatible with oxidized species (quinone-type or phenoxyl radical). These features of the peak clusters were consistent with the availability to each oligomer level of various oxidation states corresponding to sequential losses of H atoms (see ESI Section). This evidence was previously reported in the case of the oxidative polymerization of 1,8-DHN, for which the formation of stable phenoxyl radicals and quinonoid forms has been supported on the basis of laser flash photolysis experiments and computational calculations.²⁰

ARTICLE

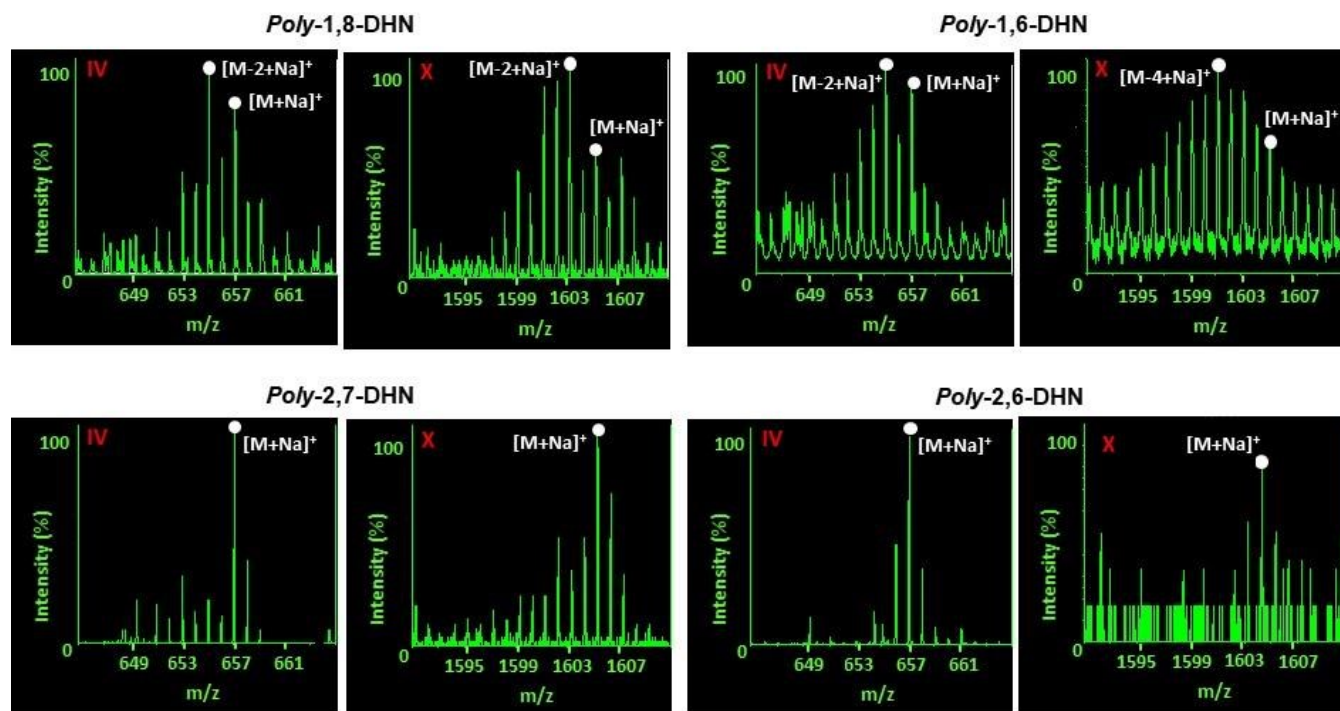


Figure 4. Comparison of the clusters of the $[M+Na]^+$ pseudomolecular ion peaks for the 4-mer (IV) and 10-mer (X) oligomeric species of synthetic melanins.

A second relevant observation in poly-1,6-DHN and poly-1,8-DHN was that cluster complexity increased with increasing oligomer molecular weight, as shown in Figure 4 when comparing the clusters of the polymer at the early stage (4-mer stage) with those of the grown polymer (10-mer stage). Finally, the relative height of the pseudomolecular ion peaks for the fully reduced species usually decreased with increasing molecular mass, in accord with a shift of the dominant member of the cluster toward higher oxidation levels (lower m/z values). Overall these data indicated that higher oxidation levels with higher degrees of electronic/redox disorder become prevailing at higher levels of polymerization. A lesser degree of electronic/redox disorder was deduced by inspection of the clusters of poly-2,7-DHN and poly-2,6-DHN, for which ion peaks for the fully reduced state prevailed at each oligomeric stage. Consistent with the above data, the mass spectra of the films registered in the MALDI mode confirmed the main features of the polymers in the bulk form (see ESI section). The dominant peaks were assigned to singly-charged distributions, up to 15 repeating units in the case of 1,8-DHN. The mass spectra of the films suggested also that the polymers formed under the AISP conditions were characterized by a more pronounced structural integrity with respect to polymers obtained by oxidative

polymerization in solution. The presence of regular clusters of peaks centered around the expected pseudomolecular ion peak confirmed a limited proportion of oxidized naphthalene units also in the solid state. All spectra confirmed moreover the lack of detectable incorporation of ammonia during exposure to the gas to promote aerial oxidation.

Given the apparently higher complexity of the oligomer clusters in those melanins which displayed the darkest colorations and the highest electron spin densities, the existence of possible correlations between melanin optical properties, spin density and redox state was finally investigated.

To this aim, the integrated areas of the featureless absorption curves of thin films in the visible region (400-800 nm) were plotted against the full width at half maximum (FWHM) measured for the Gaussian best-fit on the $[M+Na]^+$ 10-mer cluster in the MALDI mass spectra for the four melanin samples investigated. A similar plot was also generated from the electron spin density and FWHM values.

The data reported in Figure 5 indicated excellent linear correlations in both cases, supporting the view that melanin black chromophore and paramagnetic properties are prominent manifestations of redox and π -electron disorder.

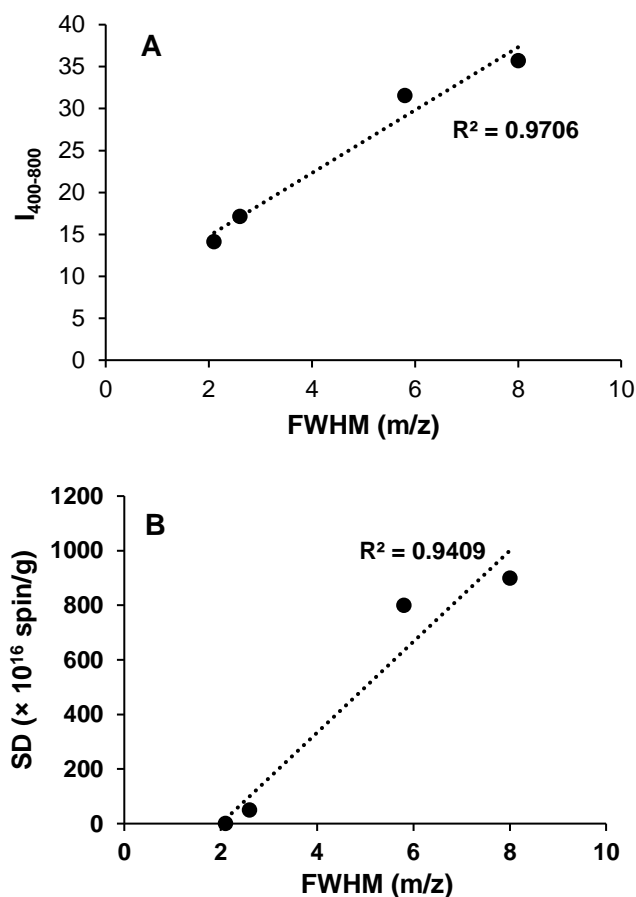


Figure 5. Trends of the integrated areas of the absorption curves of melanin thin films in the visible region (400–800 nm) from UV-vis spectra (A) and spin density (SD) from EPR spectra (B) with the full width at half maximum (FWHM) of the $[M+Na]^+$ 10-mer cluster in the MALDI mass spectra.

Although some caution needs to be exercised before taking MALDI-MS analysis as a reliable index of redox disorder, the observed broadening of peak clusters with increasing oligomer molecular weight and the consistent dominance of reduced states in the light colored melanin from 2,6-DHN would support the validity and meaningfulness of the FWHM parameter for the purposes of this study.

Conclusions

Comparative analysis of a set of synthetic melanin polymers from isomeric DHN derivatives disclosed clear-cut correlations between visible absorption properties, oligomer size, redox state dispersion and EPR spin density. It is concluded that blackness is a primary index of π -electron complexity, rather than of simple structural disorder, caused by strong intermolecular perturbations of π -electron systems within a range of redox states coexisting at each oligomer population level (Figure 6). This concept, as corroborated by on-going studies on structure-property relationships in complex redox organic polymers, may open new vistas on the way to a systems chemistry entry to melanin-type functional materials for tailored applications.

Conflicts of interest

The authors declare that there are no conflicts.

Acknowledgements

This work was supported in part by Italian MIUR grants PRIN 2017YJMPZN to Mdl and 2017CBHCWF_003 to PM.

References

- 1 A. B. Mostert, S. B. Rienecker, C. Noble, G. R. Hanson and P. Meredith, *Sci. Adv.* 2018, **4**, eaaq1293.
- 2 L. Panzella, G. Gentile, G. D'Errico, N. F. Della Vecchia, M. E. Errico, A. Napolitano, C. Carfagna and M. d'Ischia, *Angew. Chem. Int. Ed.* 2013, **52**, 12684–12687.
- 3 R. Micillo, M. Iacomino, M. Perfetti, L. Panzella, K. Koike, G. D'Errico, M. d'Ischia and A. Napolitano, *Pigment Cell Melanoma Res.* 2018, **31**, 475–483.
- 4 P. Manini, L. Panzella, T. Eidenberger, A. Giarra, P. Cerruti, M. Trifuoggi and A. Napolitano, *J. Agric. Food Chem.* 2016, **64**, 890–897.
- 5 S. R. Cicco, M. Ambrico, P. F. Ambrico, M. Mastropasqua Talamo, A. Cardone, T. Ligonzo, R. Di Mundo, C. Giannini, T. Sibillano, G. M. Farinola, P. Manini, A. Napolitano, V. Criscuolo and M. d'Ischia, *J. Mater. Chem. C* 2015, **3**, 2810–2816.
- 6 M. d'Ischia, K. Wakamatsu, F. Cicoira, E. Di Mauro, J. C. Garcia-Borron, S. Commo, I. Galván, G. Ghanem, K. Kenzo, P. Meredith, A. Pezzella, C. Santato, T. Sarna, J. D. Simon, L. Zecca, F. A. Zucca, A. Napolitano and S. Ito, *Pigment Cell Melanoma Res.* 2015, **28**, 520–544.
- 7 Z. Wang, Y. Zou, Y. Li and Y. Cheng, *Small* 2020, **16**, 1907042.
- 8 P. Yang, S. Zhang, X. Chen, X. Liu, Z. Wang and Y. Li, *Mater. Horiz.*, 2020, **7**, 746–761.
- 9 P. Yang, Z. Gu, F. Zhu and Y. Li, *CCS Chem.* 2020, **2**, 128–138.
- 10 B.-L. L. Seagle, K. A. Rezai, Y. Kobori, E. M. Gasyna, K. A. Rezaei and J. R. Jr Norris, *Proc. Natl. Acad. Sci. USA* 2005, **102**, 8978–8983.
- 11 C. Pacelli, R. A. Bryan, S. Onofri, L. Selbmann, L. Zucconi, I. Shuryak and E. Dadachova, *Environ. Microbiol. Rep.* 2018, **10**, 255–263.
- 12 A. A. R. Watt, J. P. Bothma and P. Meredith, *Soft Matter* 2009, **5**, 3754–3760.
- 13 M. d'Ischia, A. Napolitano, A. Pezzella, P. Meredith and T. Sarna, *Angew. Chem. Int. Ed.* 2009, **48**, 3914–3921.
- 14 A. Pezzella, A. Iadonisi, S. Valerio, L. Panzella, A. Napolitano, M. Adinolfi and M. d'Ischia, *J. Am. Chem. Soc.* 2009, **131**, 15270–15275.
- 15 C. Bonavolontà, C. de Lisio, M. d'Ischia, P. Maddalena, P. Manini, A. Pezzella and M. Valentino, *Sci. Rep.* 2017, **7**, 1–8.
- 16 C.-T. Chen, C. Chuang, J. Cao, V. Ball, D. Ruchand M. J. Buehler, *Nat. Commun.* 2014, **5**, 3859.
- 17 F. R. Kohl, C. Grieco and B. Kohler, *Chem. Sci.* 2020, **11**, 1248–1259.
- 18 P. Manini, V. Lino, P. Franchi, G. Gentile, T. Sibillano, C. Giannini, E. Picardi, A. Napolitano, L. Valgimigli, C. Chiappe and M. d'Ischia, *ChemPlusChem* 2019, **84**, 1331–1337.
- 19 M. M. Cecchini, S. Reale, P. Manini, M. d'Ischia and F. De Angelis, *Chem. Eur. J.* 2017, **23**, 8092–8098.
- 20 P. Manini, M. Bietti, M. Galeotti, M. Salamone, O. Lanzalunga, M. M. Cecchini, S. Reale, O. Crescenzi, A.

- Napolitano, F. De Angelis, V. Barone and M. d'Ischia, *ACS Omega* 2018, **3**, 3918–3927.
- 21 M. d'Ischia, A. Napolitano, A. Pezzella, P. Meredith, M. J. Buehler, *Angew. Chem. Int. Ed.* 2019, DOI: 10.1002/anie.201914276.
- 22 P. Manini, V. Lucci, V. Lino, S. Sartini, F. Rossella, G. Falco, C. Chiappe, M. d'Ischia, *J. Mater. Chem. B* 2020, **8**, 4412–4418.
- 23 A. Pezzella, M. Barra, A. Musto, A. Navarra, M. Alfè, P. Manini, S. Parisi, A. Cassinese, V. Criscuolo and M. d'Ischia, *Mater. Horiz.* 2015, **2**, 212–220.
- 24 M. J. Beltrán-García, F. M. Prado, M. S. Oliveira, D. Ortiz-Mendoza, A. C. Scalfo, A. Pessoa Jr, M. H. G. Medeiros, F. White and P. Di Mascio, *PLoS ONE* 2014, **9**, e91616.
- 25 S. Reale, M. Crucianelli, A. Pezzella, M. d'Ischia and F. De Angelis, *J. Mass. Spectrom.* 2012, **47**, 49–53.
- 26 A. Napolitano, A. Pezzella, G. Prota, R. Seraglia and P. Traldi, *Rapid Commun. Mass Spectrom.* 1996, **10**, 204–208.
- 27 A. Napolitano, A. Pezzella, G. Prota, R. Seraglia and P. Traldi, *Rapid Commun. Mass Spectrom.* 1996, **10**, 468–472.

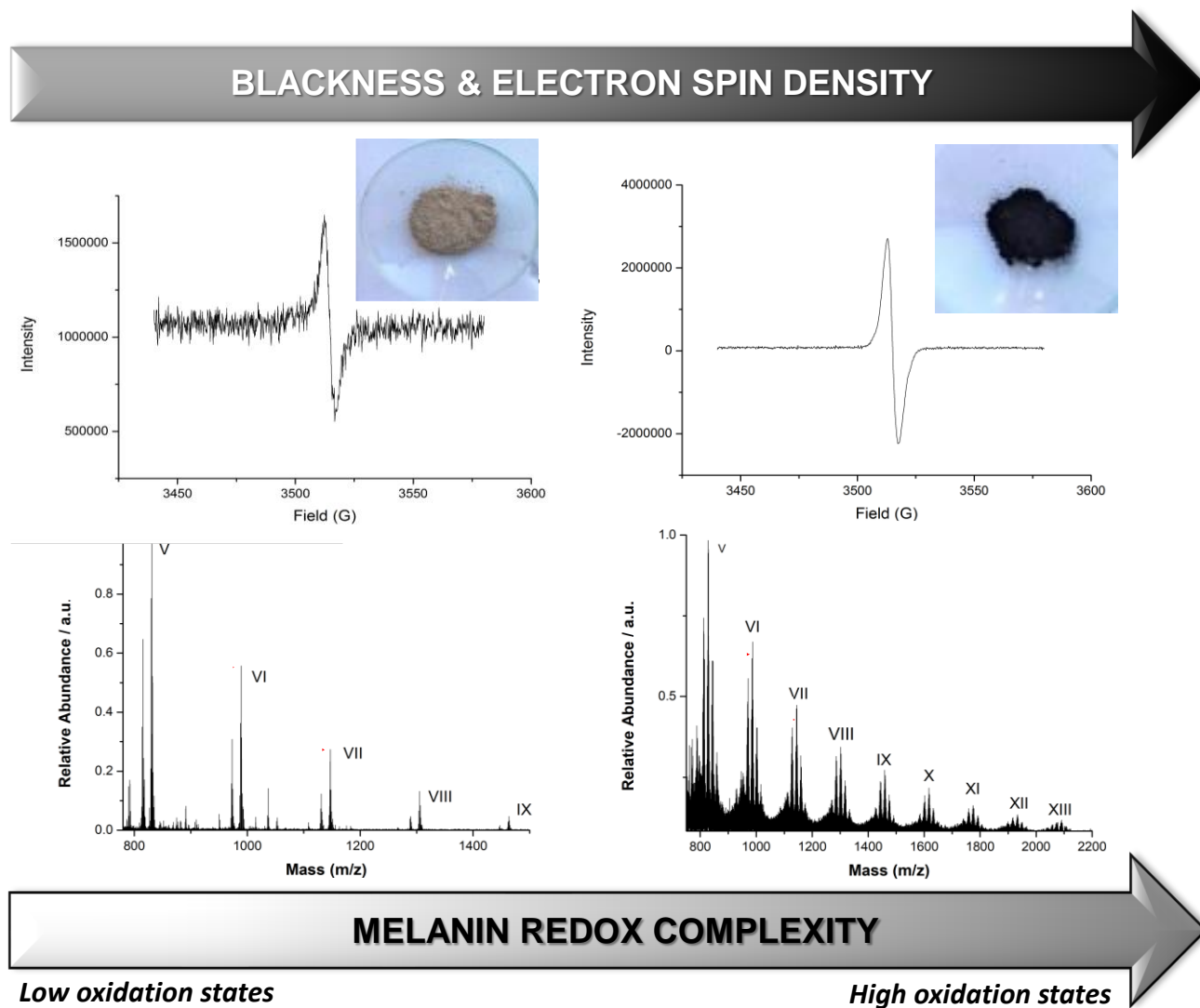


Figure 6. Schematic representation of the correlation between blackness and redox state disorder in melanin polymers.

